Numerical Assignment

Mariana Clare

November 9, 2017

1 Defining Shallow Water Equations

The shallow water equations are

$$\frac{\partial \mathbf{u}}{\partial t} + \mathbf{u} \cdot \nabla \mathbf{u} = -2\Omega \times \mathbf{u} - g\nabla(h + h_0) \tag{1}$$

$$\frac{\partial h}{\partial t} + \mathbf{u} \cdot \nabla h = -h\nabla \cdot \mathbf{u} \tag{2}$$

where $\mathbf{u}$ is the velocity of the flow, Ω is the angular velocity of the rotating frame of reference, g is the gravitational acceleration constant, h is the depth of the fluid and h_0 represents the underlying shape that the fluid is flowing over (as defined in [1]).

The first equation (1) represents the conservation of momentum and the second equation (2) represents the conservation of mass. Both equations have a $u \cdot \nabla$ which represents advection.

In order to solve these equations numerically, they first need to be linearised about the state $u = 0$ and $h = H$ ie.

$$\begin{aligned} \mathbf{u} &= \quad \hat{\mathbf{u}} \\ h &= \quad H + \hat{h}. \end{aligned}$$

where H is the average fluid depth. If we further assume that h_0 is constant, this gives

$$\frac{\partial \hat{\mathbf{u}}}{\partial t} = 2\Omega \times \hat{\mathbf{u}} - g\nabla\hat{h} \tag{3}$$

$$\frac{\partial \hat{h}}{\partial t} = -H\nabla \cdot \hat{\mathbf{u}} \tag{4}$$

These equations can be simplified further by assuming there is no rotation and taking the one-dimensional form. Dropping the $\hat{}$ notation this gives

$$\frac{\partial u}{\partial t} = -g\frac{\partial h}{\partial x} \tag{5}$$

$$\frac{\partial h}{\partial t} = -H\frac{\partial u}{\partial x}. \tag{6}$$

This report will seek to solve these one-dimensional lineriased shallow water equations numerically. Note that throughout this report we will assume for simplicity that u and h have periodic boundary conditions.

2 Numerical Methods

The first numerical method we use to attempt to solve (5) and (6) is a simple co-located forward-backward in time and centred in space scheme. As in [1], we consider the scheme to be forward in u and backward in h. Co-located means we define the velocity and the height at the same location in space on the meshgrid and these schemes are also referred to as A-grid or unstaggered schemes.

This scheme can be written as

$$\frac{u_j^{(n+1)} - u_j^{(n)}}{\Delta t} = -g\frac{h_{j+1}^{(n)} - h_{j-1}^{(n)}}{2\Delta x} \tag{7}$$

$$\frac{h_j^{(n+1)} - h_j^{(n)}}{\Delta t} = -H\frac{u_{j+1}^{(n+1)} - u_{j-1}^{(n+1)}}{2\Delta x} \tag{8}$$

where $h_j^{(n)} = h(x_j, t^{(n)})$, $u_j^{(n)} = h(u_j, t^{(n)})$, $x_j = j\Delta x$ and $t^{(n)} = n\Delta t$.

We can determine the order of accuracy of this scheme, by using Taylor series. We note the following Taylor series expansions:

$$u_j^{(n+1)} = u_j^{(n)} + \Delta t\frac{\partial u_j^{(n)}}{\partial t} + \frac{(\Delta t)^2}{2}\frac{\partial^2 u_j^{(n)}}{\partial t^2} + O((\Delta t)^3) \tag{9}$$

$$h_{j\pm1}^{(n)} = h_j^{(n)} \pm \Delta x\frac{\partial h_j^{(n)}}{\partial x} + \frac{(\Delta x)^2}{2}\frac{\partial^2 h_j^{(n)}}{\partial x^2} \pm \frac{(\Delta x)^3}{6}\frac{\partial^3 h_j^{(n)}}{\partial x^3} + O((\Delta x)^4) \tag{10}$$

Substuting these expansions into the scheme (7), we find that

$$\frac{\partial u_j^{(n)}}{\partial t} + O(\Delta t) = -g\frac{\partial h_j^{(n)}}{\partial x} + O((\Delta x)^2) \tag{11}$$

and therefore the scheme is first order accurate in time and second order accurate in space. (Note the same order of accuracy is obtained by performing the same analysis with (8)).

In order to find when this scheme is stable, we use a von-neumann stability analysis. As in [1], we assume that u and h have wave-like solutions with an amplification factor A and wavenumber k:

$$u = \mathbb{U}A^n e^{ikj\Delta x} \tag{12}$$

$$h = \mathbb{H}A^n e^{ikj\Delta x} \tag{13}$$

for constant $\mathbb{U}$ and $\mathbb{H}$.

Further if we define the courant number

$$c = \frac{\sqrt{gH}\Delta t}{\Delta x} \tag{14}$$

then substituting these solutions into (7) and (8) gives

$$A = 1 - \frac{c^2}{2}\sin^2(k\Delta x) \pm \frac{ic}{2}\sin(k\Delta x)\sqrt{4 - c^2\sin^2 k\Delta x}. \tag{15}$$

Hence as found in [1], when $|c| \leq 2$, $|A|^2 = 1$ and the scheme is stable, but when $|c| > 2$, the scheme is unstable.

We can also find the dispersion relation, because the frequency of the numerical method is

$$\omega = \pm\frac{1}{\Delta t}\arctan\left(\frac{Im(A)}{Re(A)}\right) \tag{16}$$

Using the result from [1],

$$\omega_n \Delta x = \pm\frac{2}{c}\sin^{-1}\left(\frac{c}{2}\sin(k\Delta x)\right) \tag{17}$$

assuming $\sqrt{gH} = 1$. The positive branch of this dispersion relation is plotted in Figure 1 and compared with the dispersion relation of the analytical solution. (The dispersion relation of the analytical solution $\omega = k\sqrt{gH}$ is found by substituting the wave-like solutions (12) and (13) into (5) and (6)).

However, we would like to have a method that was stable for all courant numbers. Therefore another method we can use is an implicit method on a co-located grid. As in [1], we look at the forward in time for both u and h and centred in space co-located scheme:

$$\frac{u_j^{(n+1)} - u_j^{(n)}}{\Delta t} = -g\frac{h_{j+1}^{(n+1)} - h_{j-1}^{(n+1)}}{2\Delta x} \tag{18}$$

$$\frac{h_j^{(n+1)} - h_j^{(n)}}{\Delta t} = -H\frac{u_{j+1}^{(n+1)} - u_{j-1}^{(n+1)}}{2\Delta x}. \tag{19}$$

In order to find the values of h_j^n and u_j^n at the next time iteration for all j, we consider the matrix:

$$A = \begin{pmatrix} 1+\frac{c^2}{2} & 0 & -\frac{c^2}{4} & 0 & 0 & & 0 & 0 & 0 & -\frac{c^2}{4} & 0 \\ 0 & 1+\frac{c^2}{2} & 0 & -\frac{c^2}{4} & 0 & \vdots & 0 & 0 & 0 & 0 & -\frac{c^2}{4} \\ -\frac{c^2}{4} & 0 & 1+\frac{c^2}{2} & 0 & -\frac{c^2}{4} & \ddots & \vdots & & \vdots & & \vdots \\ \vdots & & \vdots & & \vdots & & -\frac{c^2}{4} & 0 & 1+\frac{c^2}{2} & 0 & -\frac{c^2}{4} \\ -\frac{c^2}{4} & 0 & 0 & 0 & 0 & \vdots & 0 & -\frac{c^2}{4} & 0 & 1+\frac{c^2}{2} & 0 \\ 0 & -\frac{c^2}{4} & 0 & 0 & 0 & & 0 & 0 & -\frac{c^2}{4} & 0 & 1+\frac{c^2}{2} \end{pmatrix}$$

where c is the courant number as before.

We then rewrite the scheme (18) and (19) as the matrix equation $A\mathbf{x} = \mathbf{b}$ where

$$x_j = h_j^{(n+1)} \text{ and } b_j = h_j^{(n)} - \frac{c}{2}\sqrt{\frac{H}{g}}(u_{j+1}^{(n)} - u_{j-1}^{(n)}) \qquad \forall j \in [0, N-1] \tag{20}$$

if solving for h and

$$x_j = u_j^{(n+1)} \text{ and } b_j = u_j^{(n)} - \frac{c}{2}\sqrt{\frac{g}{H}}(h_{j+1}^{(n)} - h_{j-1}^{(n)}) \qquad \forall j \in [0, N-1] \tag{21}$$

if solving for u.

Note that the matrix A has dimension $N \times N$ and we consider the first row to be $j = 0$.

Furthermore, here and throughout this report we are assuming periodic boundary conditions and hence that $u_0^{(n)} = u_N^{(n)}$ and $h_0^{(n)} = h_N^{(n)}$ where $N\Delta x$ is the right hand boundary of the x-domain. Hence the matrix A has dimension $N \times N$ and we consider the first row to be $j = 0$.

We can determine the order of accuracy of this scheme, as before by using the Taylor series expansions (9) and

$$h_{j\pm1}^{(n+1)} = h_j^{(n)} \pm \Delta x\frac{\partial h_j^{(n)}}{\partial x} + \frac{(\Delta x)^2}{2}\frac{\partial^2 h_j^{(n)}}{\partial x^2} \pm \Delta x\Delta t\frac{\partial^2 h_j^{(n)}}{\partial x \partial t} + \frac{(\Delta t)^2}{2}\frac{\partial^2 h_j^{(n)}}{\partial t^2} + O((\Delta x)^3, (\Delta t)^3). \tag{22}$$

Substituting this into equation (18) we find that

$$\frac{\partial u_j^{(n)}}{\partial t} + O(\Delta t) = -g\frac{\partial h_j^{(n)}}{\partial x} + O((\Delta x)^2). \tag{23}$$

Therefore the scheme is first order accurate in time and second order accurate in space as with the explicit method on the co-located grid. (As before a similar result can be obtained by substituting in to (19)).

In order to find where this method is stable, we use von-neumann stability analysis and assume u and h have wave-like solutions (12) and (13). Substituting these solutions into (18) and (19) we find

$$A = \frac{1 \pm ic\sin(k\Delta x)}{1 + c^2\sin^2(k\Delta x)} \tag{24}$$

Therefore

$$|A|^2 = \frac{1}{1 + c^2\sin^2(k\Delta x)} < 1 \qquad \forall k, \Delta x \tag{25}$$

and the system is stable everywhere.

Using (16) we can find the dispersion relation

$$\omega_n\Delta x = \pm\frac{\Delta x}{\Delta t}\arctan(c\sin(k\Delta x)) = \frac{1}{c}\arctan(c\sin(k\Delta x)) \tag{26}$$

assuming $\sqrt{gH} = 1$. The positive branch of this dispersion relation is again plotted in Figure 1.

We can see from this Figure 1 that the analytic solution and numerical solution do not propagate at the same rate. The numeric solution disperses too slowly and in fact at $k = \pi$, the wave is stationary.

Therefore we seek a scheme which propagates at a more similar speed to the analytic solution. Following [1], we use a staggered grid (sometimes known as a C-grid) instead of a co-located grid. For a staggered grid, we shift u so that it is defined at $x_j + \frac{\Delta x}{2}$ and h remains defined at x_j (where $x_j = j\Delta x$) ie. where u and h are defined alternates in space.

As in [1], we take again the forward-backward in time and centred in space scheme where the scheme is forward in u and backward in h, but this time on a staggered grid. This gives us the following scheme:

$$\frac{u_{j+\frac{1}{2}}^{(n+1)} - u_{j+\frac{1}{2}}^{(n)}}{\Delta t} = -g\frac{h_{j+1}^{(n)} - h_j^{(n)}}{\Delta x} \tag{27}$$

$$\frac{h_j^{(n+1)} - h_j^{(n)}}{\Delta t} = -H\frac{u_{j+\frac{1}{2}}^{(n+1)} - u_{j-\frac{1}{2}}^{(n+1)}}{\Delta x} \tag{28}$$

We can determine the order of accuracy of this scheme, as before, by using the Taylor series expansions (10) and

$$u_{j\pm\frac{1}{2}}^{(n)} = u_j^{(n)} \pm \frac{\Delta x}{2}\frac{\partial u_j^{(n)}}{\partial x} + \frac{(\Delta x)^2}{8}\frac{\partial^2 u_j^n}{\partial x^2} + O((\Delta x)^3. \tag{29}$$

$$u_{j\pm\frac{1}{2}}^{(n+1)} = u_j^{(n)} \pm \frac{\Delta x}{2}\frac{\partial u_j^{(n)}}{\partial x} + \Delta t\frac{\partial u_j^{(n)}}{\partial t} + \frac{(\Delta x)^2}{8}\frac{\partial^2 u_j^n}{\partial x^2} \pm \frac{\Delta t\Delta x}{2}\frac{\partial^2 u_j^{(n)}}{\partial x\partial t} + \frac{(\Delta t)^2}{2}\frac{\partial^2 u_j^{(n)}}{\partial t^2} + O((\Delta x)^3, (\Delta t)^3) \tag{30}$$

Substituting these into (27), we find that

$$\frac{\partial u_j^{(n)}}{\partial t} + O(\Delta t) = -g\frac{\partial h_j^{(n)}}{\partial x} + O((\Delta x)^2) \tag{31}$$

and therefore the scheme is first order accurate in time and second order accurate in space. (Note as before the same order of accuracy is obtained by performing the same analysis with (28)).

In order to find where this method is stable, we use von-neumann stability analysis and assume u and h have wave-like solutions (12) and (13). Substituting these solutions into (27) and (28) we find

$$A = 1 - 2c^2\sin^2\left(\frac{k\Delta x}{2}\right) \pm 2ic\sin\left(\frac{k\Delta x}{2}\right)\sqrt{1 - c^2\sin^2(\frac{k\Delta x}{2}\right)} \tag{32}$$

Therefore if $|c| \leq 1$, this scheme is stable, but if $|c| > 1$ the scheme is unstable.

Using (16) we can find the dispersion relation

$$\omega_n \Delta x = \pm \frac{2\Delta x}{\Delta t} \arcsin\left(c \sin\left(\frac{k\Delta x}{2}\right)\right) = \frac{2}{c} \arcsin\left(c \sin\left(\frac{k\Delta x}{2}\right)\right) \tag{33}$$

assuming $\sqrt{gH} = 1$. The positive branch of this dispersion relation is again plotted in Figure 1.

Although this solution is still dispersive we can see from the Figure that ω of this numeric scheme is much closer to ω of the analytic solution.

However we again have the problem that the solution is unstable. Therefore the final numerical scheme we will look at is the semi-implicit scheme on a staggered grid outlined in [2].

The scheme used in [2] is the theta-method:

$$\frac{u_{j+\frac{1}{2}}^{(n+1)} - u_{j+\frac{1}{2}}^{(n)}}{\Delta t} = -\frac{g}{\Delta x}\left(\theta(h_{j+1}^{(n+1)} - h_j^{(n+1)}) + (1-\theta)(h_{j+1}^{(n)} - h_j^{(n)})\right) \tag{34}$$

$$\frac{h_j^{(n+1)} - h_j^{(n)}}{\Delta t} = -\frac{H}{\Delta x}\left(\theta(u_{j+\frac{1}{2}}^{(n+1)} - u_{j-\frac{1}{2}}^{(n+1)}) + (1-\theta)(u_{j+\frac{1}{2}}^{(n)} - u_{j-\frac{1}{2}}^{(n)})\right) \tag{35}$$

For simplicity we have taken $\theta = \frac{1}{2}$ and are therefore using the Crank-Nicholson method centred in space on a staggered grid:

$$\frac{u_{j+\frac{1}{2}}^{(n+1)} - u_{j+\frac{1}{2}}^{(n)}}{\Delta t} = -\frac{g}{2\Delta x}\left((h_{j+1}^{(n+1)} - h_j^{(n+1)}) + (h_{j+1}^{(n)} - h_j^{(n)})\right) \tag{36}$$

$$\frac{h_j^{(n+1)} - h_j^{(n)}}{\Delta t} = -\frac{H}{2\Delta x}\left((u_{j+\frac{1}{2}}^{(n+1)} - u_{j-\frac{1}{2}}^{(n+1)}) + (u_{j+\frac{1}{2}}^{(n)} - u_{j-\frac{1}{2}}^{(n)})\right) \tag{37}$$

In order to find the values of h_j^n and u_j^n at the next time iteration for all j, we consider the matrix:

$$A = \begin{pmatrix} 1+\frac{c^2}{2} & -\frac{c^2}{4} & 0 & & 0 & 0 & -\frac{c^2}{4} \\ -\frac{c^2}{4} & 1+\frac{c^2}{2} & -\frac{c^2}{4} & \vdots & 0 & 0 & 0 \\ \vdots & \vdots & \vdots & \ddots & \vdots & \vdots & \vdots \\ 0 & 0 & 0 & \vdots & -\frac{c^2}{4} & 1+\frac{c^2}{2} & -\frac{c^2}{4} \\ -\frac{c^2}{4} & 0 & 0 & & 0 & -\frac{c^2}{4} & 1+\frac{c^2}{2} \end{pmatrix}$$

where c is the courant number as before.

We then rewrite the scheme (36) and (37) as the matrix equation $A\mathbf{x} = \mathbf{b}$.

$$x_j = h_j^{(n+1)} \text{ and } b_j = -c\sqrt{\frac{g}{H}}(h_{j+1}^{(n)} - h_j^n) + \frac{c^2}{4}u_{j+\frac{3}{2}}^{(n)} + (1-\frac{c^2}{2})u_{j+\frac{1}{2}}^{(n)} + \frac{c^2}{4}u_{j-\frac{1}{2}}^{(n)} \qquad \forall j \in [0, N-1] \tag{38}$$

if solving for h and

$$x_j = u_{j+\frac{1}{2}}^{(n+1)} \text{ and } b_j = -c\sqrt{\frac{H}{g}}(u_{j+\frac{1}{2}}^{(n)} - u_{j-\frac{1}{2}}^n) + \frac{c^2}{4}h_{j+1}^{(n)} + (1-\frac{c^2}{2})h_j^{(n)} + \frac{c^2}{4}h_{j-1}^{(n)} \qquad \forall j \in [0, N-1] \tag{39}$$

if solving for u.

Note that the matrix A has dimension $N \times N$ and we consider the first row to be $j = 0$.

Furthermore as before we have assumed periodic boundary conditions and hence that $u_{\frac{1}{2}}^{(n)} = u_{N+\frac{1}{2}}^{(n)}$ and $h_0^{(n)} = h_N^{(n)}$ where $N\Delta x$ is the right hand boundary of the x-domain.

We can determine the order of accuracy of this scheme, as before by using the Taylor series expansions (29) and (30) and

$$h_j^{(n+1)} = h_j^{(n)} + \Delta t\frac{\partial h_j^{(n)}}{\partial t} + \frac{(\Delta t)^2}{2}\frac{\partial^2 h_j^{(n)}}{\partial t^2} + O((\Delta t)^3). \tag{40}$$

Substituting these into (37) we find that

$$\frac{\partial h_j^{(n)}}{\partial t} + O((\Delta t)^2) = -H\frac{\partial u_j^{(n)}}{\partial x} + O((\Delta x)^2) \tag{41}$$

and therefore the scheme is second order accurate in time and second order accurate in space which is better than any of the other schemes we have looked at so far. (Note as before the same order of accuracy is obtained by performing the same analysis with (36)).

As before in order to find where this method is stable, we use von-neumann stability analysis and assume u and h have wave-like solutions (12) and (13). Substituting these solutions into (36) and (37) we find:

$$A = \frac{2 - 2c^2\sin^2(\frac{k\Delta x}{2}) \pm 4ic\sin(\frac{k\Delta x}{2})}{2 + 2c^2\sin^2(\frac{k\Delta x}{2})} \tag{42}$$

$|A|^2 = 1$ and therefore the scheme is stable and undamping $\forall k$.

Using (16) we can find the dispersion relation

$$\omega_n\Delta x = \pm\frac{\Delta x}{\Delta t}\arctan\left(\frac{2c\sin(\frac{k\Delta x}{2})}{1 - c^2\sin^2(\frac{k\Delta x}{2})}\right) = \pm\frac{1}{c}\arctan\left(\frac{2c\sin(\frac{k\Delta x}{2})}{1 - c^2\sin^2(\frac{k\Delta x}{2})}\right) \tag{43}$$

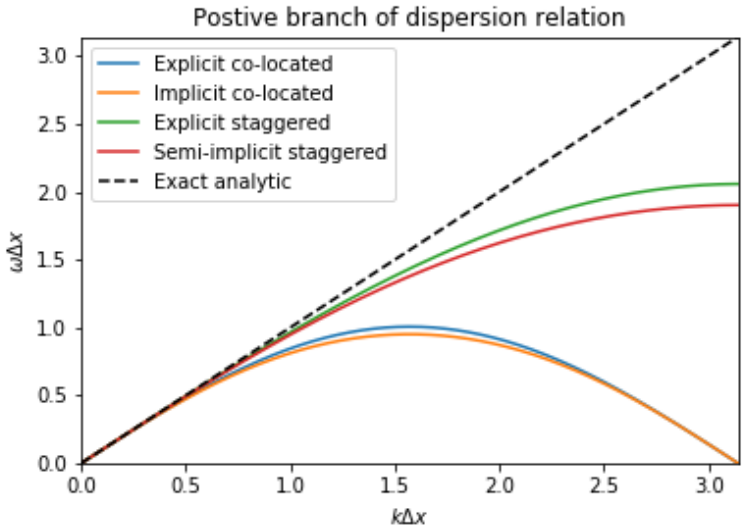

Figure 1: Postive branch of dispersion relation ω for analytic solution and numerical schemes. Note that as in [1], we have used $c = 0.4$ and $\sqrt{gH} = 1$.

assuming $\sqrt{gH} = 1$. The positive branch of this dispersion relation is again plotted in Figure 1.

As with the previous staggered grid scheme, this solution is still dispersive. The dispersion relation for the semi-implicit staggered scheme diverges more from the analytic solution than the explicit staggered scheme but it is still significantly better than either of the co-located schemes.

3 Methodology to test Numerical Methods

In order to test the properties of the Numerical methods outlined in the above section we have devised a series of tests.

3.1 Test 1

To begin with, we attempt to solve the shallow water equations using a simple initial condition (shown in Figure 2a) with the co-located forward-backward explicit scheme.

3.2 Test 2

We found using Von-Neumann stability analysis the co-located forward-backward explicit scheme is unstable for courant numbers higher than 2. Therefore we test to see if this is in fact the case.

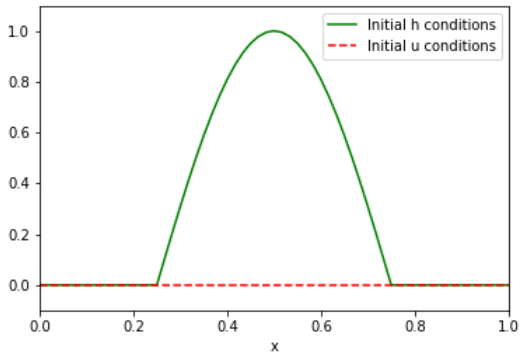

Figure 2a: Initial condition such that u is zero everywhere and h has a bump in the centre with zero either side (hereafter referred to as cosbell)

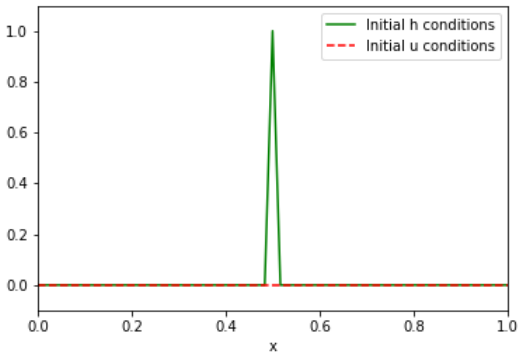

Figure 2b: Initial condition such that u is zero everywhere and h is zero everywhere apart from one point at the centre where it is one

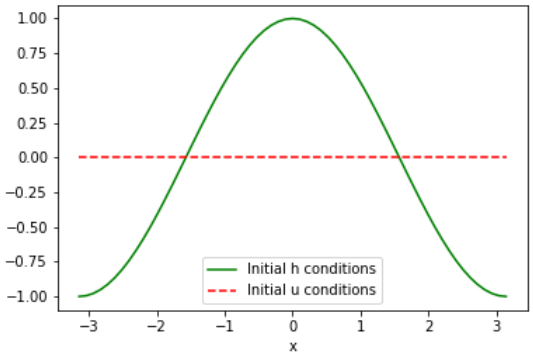

Figure 2c: Initial condition such that u is zero everywhere and h is $\cos(x)$

3.3 Test 3

We found using Von-Neumann stability analysis the co-located forward-backward implicit scheme is stable for all courant numbers. Therefore we test to see if this is in fact the case.

3.4 Test 4

When looking at the dispersion relation for the co-located grid it seems that the results produced by the scheme may be unphysical. We test this hypothesis by taking a different initial condition (shown in Figure 2b) and plotting the solutions of u and h at multiple time steps for the co-located forward-backward explicit scheme and the co-located forward-backward implicit scheme.

3.5 Test 5

Our analysis of the dispersion relations suggests that on a staggered grid the solutions for u and h should be more physical. Therefore we repeat test 3 with the same initial conditions (shown in Figure 2b), but instead using the staggered explicit scheme.

3.6 Test 6

So far all the comparisons have been about the properties of the schemes themselves. If the initial condition shown in Figure 2c is chosen it is possible to find an analytic solution of the shallow water equations

$$u = \sin(x)\sin(t) \tag{44}$$

$$h = \cos(x)\cos(t). \tag{45}$$

If we choose the interval $[-\pi, \pi]$ then these solutions are periodic.

This test will look at the solution errors between the solutions produced by the numerical scheme and the analytic solution. Note these are not the same as the errors calculated before, which are truncation errors.

3.7 Test 7

Finally we compare the computational cost of the four schemes, by comparing the time it takes for each scheme to run, starting from the same initial condition (shown in Figure 2c) and with the same number of time steps and space steps.

4 Results

For all the following results, unless otherwise explicitily stated, assume the domain used was $0 \leq x \leq 1$ and that the following parameters were used:

$$c = 0.1 \tag{46}$$
$$H = 1 \tag{47}$$
$$g = 1 \tag{48}$$
$$nx = 60 \tag{49}$$
$$nt = 100 \tag{50}$$

where c is the courant number, H is the average fluid depth, g is the gravitational acceleration constant, nx is the number of space-steps in the meshgrid and nt is the number of time-steps.

4.1 Test 1

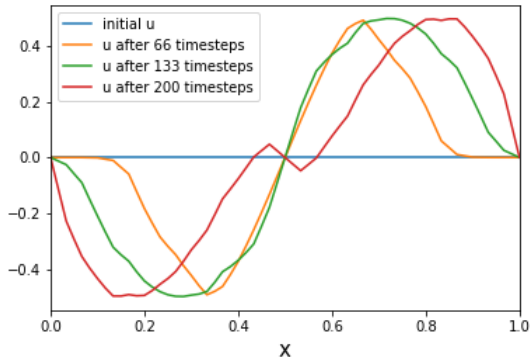

Figure 3a: Velocity at different timesteps using the co-located explicit method using the initial condition u equals 0 and h is a cosbell (as shown in Figure 2a).

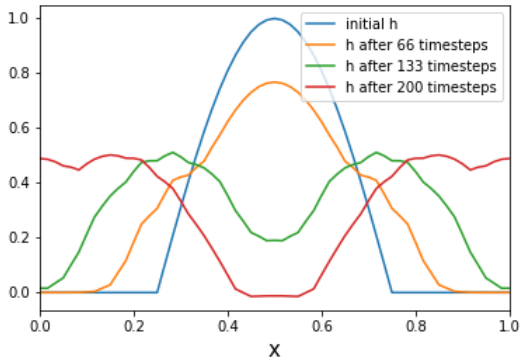

Figure 3b: Height at different timesteps using the co-located explicit method using the initial condition u equals 0 and h is a cosbell (as shown in Figure 2a).

In this test we have successfully shown that we can use the co-located explicit schemes to solve the shallow water equations. These solutions seem to make physical sense as in Figure 3b we can see fluid falling from a peak and then breaking apart over time as we would expect.

4.2 Test 2

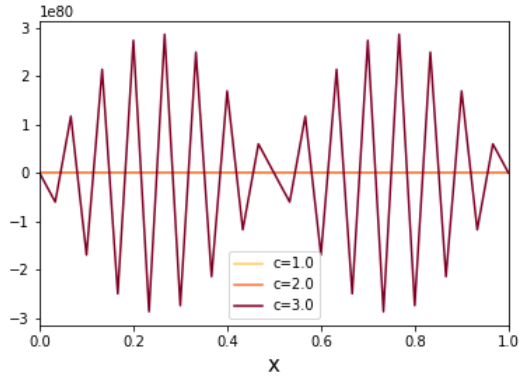

Figure 4a: Velocity for varying courant numbers for the co-located explicit method

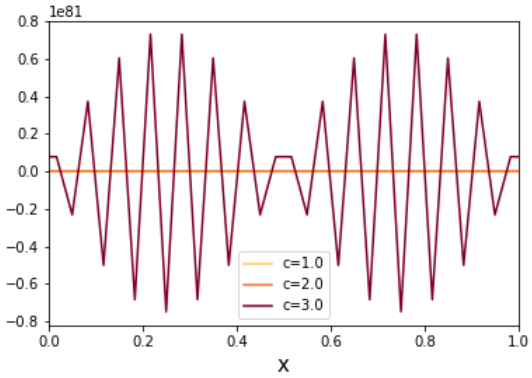

Figure 4b: Height for varying courant numbers for the co-located explicit method

Figure 4a and Figure 4b show that for large courant numbers, u and h are very unstable as we expected from the von neumann stability analysis, reaching values of an order of magnitude of 10^{80}.

4.3 Test 3

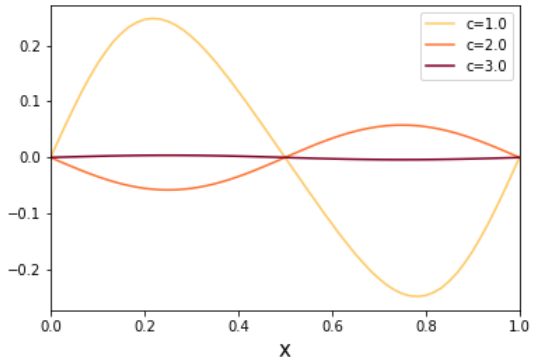

Figure 5a: Velocity for varying courant numbers for the co-located implicit method

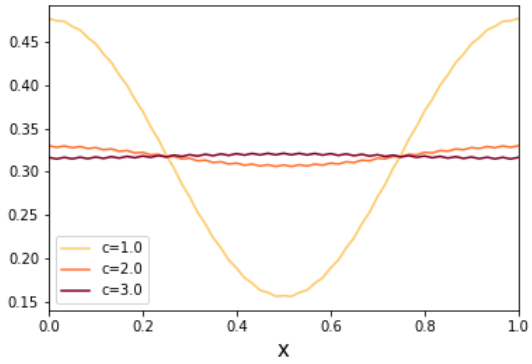

Figure 5b: Height for varying courant numbers for the co-located implicit method

By contrast with the co-located explicit method tested in section 4.2, Figure 5a and Figure 5b show that for large courant numbers, u and h remain stable as we expected from the von neumann stability analysis.

4.4 Test 4

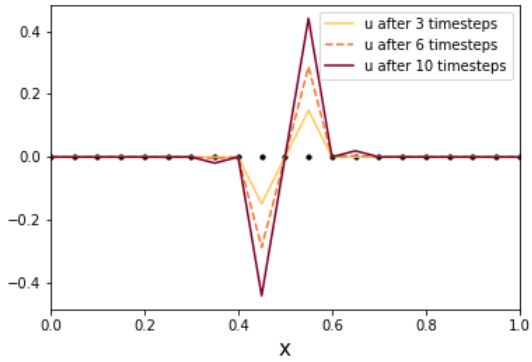

Figure 6a: Velocity at different timesteps using the co-located explicit method using the initial condition u equals 0 and h is a spike (as shown in Figure 2b). Note here we have used $nx = 20$ and $nt = 10$ (all other parameters remain the same)

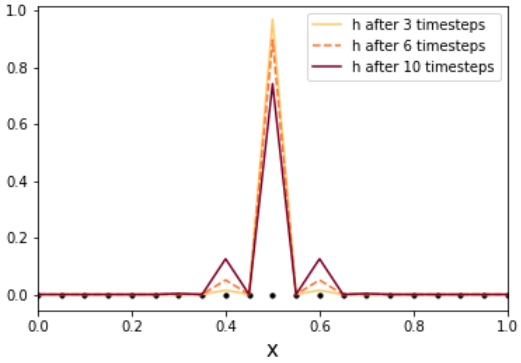

Figure 6b: Height at different timesteps using the co-located explicit method using the initial condition u equals 0 and h is a spike (as shown in Figure 2b). Note here we have used $nx = 20$ and $nt = 10$ (all other parameters remain the same)

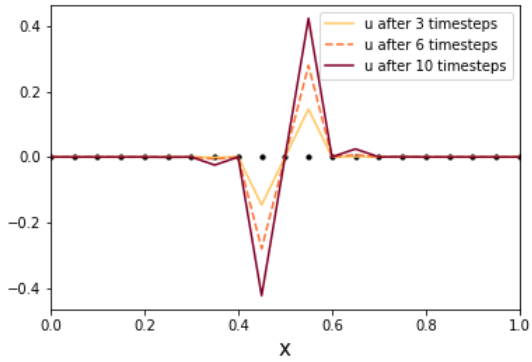

Figure 7a: Velocity at different timesteps using the co-located implicit method using the initial condition u equals 0 and h is a spike (as shown in Figure 2b). Note here we have used $nx = 20$ and $nt = 10$ (all other parameters remain the same)

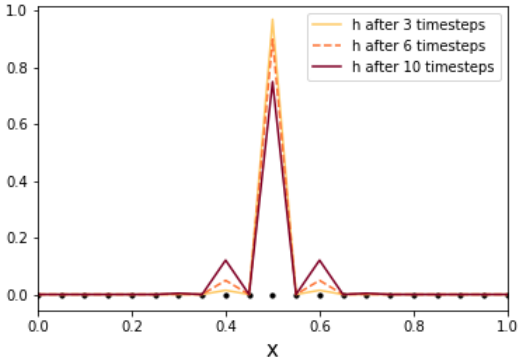

Figure 7b: Height at different timesteps using the co-located implicit method using the initial condition u equals 0 and h is a spike (as shown in Figure 2b). Note here we have used $nx = 20$ and $nt = 10$ (all other parameters remain the same)

As expected the results shown in Figures 6a, 6b, 7a and 7b are unphysical. The fluid does spread out but it does not go to the next meshpoint, instead skipping this meshpoint out and moving to the next meshpoint along. In Figure 6b and 7b, we see that the two points around the central grid point (hereafter referred to as x_m) never have any height so the fluid passes from x_m to x_{m-2} and x_{m+2} without passing through x_{m-1} and x_{m+1}

which is clearly unphysical. Similarly in Figure 6a and 7a there is never any velocity at the gridpoints x_{m-2} and x_{m+2} which is again unphysical.

Therefore our hypothesis that the results may be unphysical is true.

4.5 Test 5

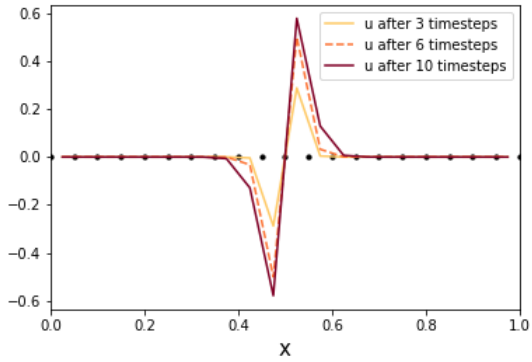

Figure 8a: Velocity at different timesteps using the staggered explicit method using the initial condition u equals 0 and h is a spike (as shown in Figure 2b). Note here we have used $nx = 20$ and $nt = 10$ (all other parameters remain the same)

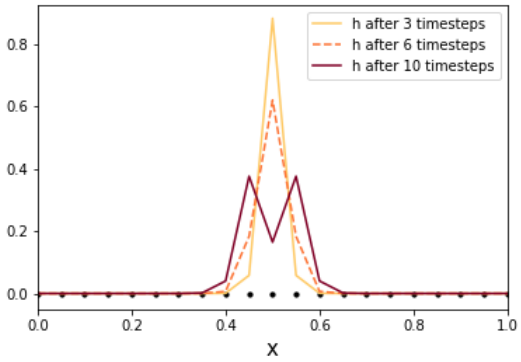

Figure 8b: Height at different timesteps using the staggered explicit method using the initial condition u equals 0 and h is a spike (as shown in Figure 2b). Note here we have used $nx = 20$ and $nt = 10$ (all other parameters remain the same)

As expected in contrast to the results in the previous test (4.4), the staggered scheme produces physical results for this initial condition. Figure 8b shows that the height spreads out evenly using all grid points. Figure 8a shows further that the velocity is non-zero at the gridpoints where the wave has so far propagated as we would expect in a physically realistic system.

4.6 Test 6

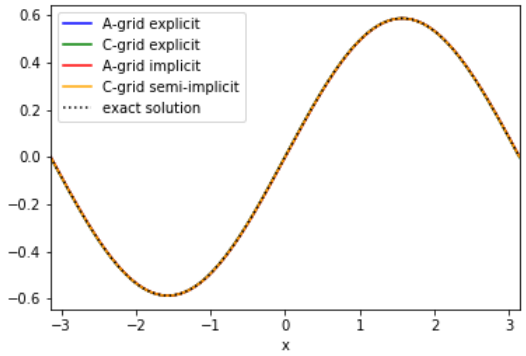

Figure 9a: Velocity, u, for the initial condition where u is 0 everywhere and h is $\cos(x)$ (as shown in Figure 2c). Note here we have used $c = 1$, $nx = 1000$, $nt = 1000$ and the domain $= \pi \leq x \leq \pi$.

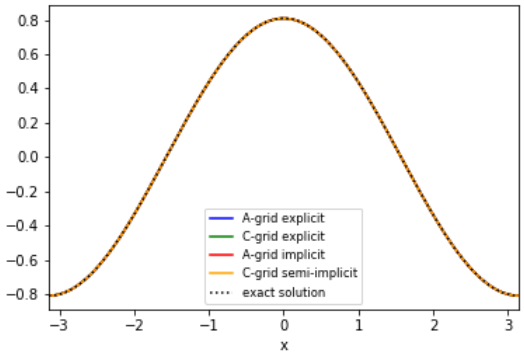

Figure 9b: Height, h, for the initial condition where u is 0 everywhere and h is $\cos(x)$ (as shown in Figure 2c). Note here we have used $c = 1$, $nx = 1000$, $nt = 1000$ and the domain $= \pi \leq x \leq \pi$.

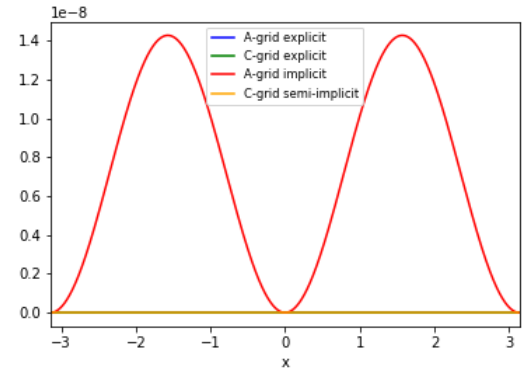

Figure 10a: Error in velocity, for the initial condition where u is 0 everywhere and h is $\cos(x)$ (as shown in Figure 2c). Note here we have used $c = 1$, $nx = 1000$, $nt = 1000$ and the domain $= \pi \leq x \leq \pi$.

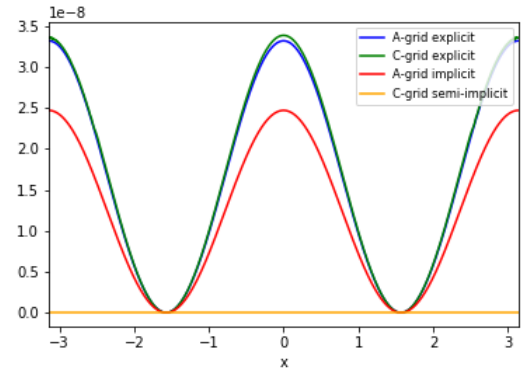

Figure 10b: Error in height, for the initial condition where u is 0 everywhere and h is $\cos(x)$ (as shown in Figure 2c). Note here we have used $c = 1$, $nx = 1000$, $nt = 1000$ and the domain $= \pi \leq x \leq \pi$.

Numerical Scheme	**Error in u**	**Error in h**
Co-located Explicit	7.4×10^{-5}	0.0041
Staggered Explicit	2.0×10^{-5}	0.0041
Co-located Implicit	0.0027	0.0035
Staggered Semi-implicit	1.9×10^{-5}	1.39×10^{-5}

Table 1

4.7 Test 7

Numerical Scheme	Time (3sf)
Co-located Explicit	2.07 s
Staggered Explicit	1.96 s
Co-located Implicit	3.23 s
Staggered Semi-implicit	84.5 s

Table 2: Time taken for each numerical scheme to run for the initial condition that h is $\cos(x)$ and u is 0 (as shown in Figure 2c) and the number of space steps is 1000 and number of time steps is 1000.

5 Conclusions

From the results listed in Section 4, we can conclude the following:

- Staggered grids produce more physically realistic results than co-located grids for certain initial conditions (from Test 4 and Test 5)
- When working with high courant numbers (e.g. if the meshgrid spacing is very fine so Δx is small or if H or Δt are very large), it is better to choose implicit methods as they are stable for all courant numbers whereas explicit methods can have large instabilities (from Test 2 and Test 3)
- SOME COMMENT ABOUT ERRORS
- When working with small courant numbers, it is better to choose explicit methods as they are much less computationally expensive than implicit methods (from Test 7)

References

[1] Cotter, C. and Weller, H., (2018), 'Numerical Methods', Ch.5 in Crisan, D (eds.), *Mathematics of Planet Earth: a primer*, World Scientific Publishing Europe Ltd., London.

[2] Casulli, V. and Cattani, E., (1994), 'Stability, Accuracy and Efficiency of a Semi-Implicit Method for Three-Dimensional Shallow Water Flow', *Computers Math. Applic*, **27(4)**, 99-112.